Production of iodine atoms by RF discharge decomposition of CF3I

Vít Jirásek, Josef Schmiedberger, Miroslav Čenský, Jarmila Kodymová

Production of iodine atoms by RF discharge decomposition of CF_3I

Vít Jirásek, Josef Schmiedberger, Miroslav Čenský, and Jarmila Kodymová

Institute of Physics, v.v.i., Academy of Sciences of the Czech Republic, Na Slovance 2, 18221 Prague, Czech Republic

E-mail: jirasek@fzu.cz

Abstract

A generation of atomic iodine by dissociation of CF_3I in RF discharge was studied experimentally in a configuration ready for direct use of the method in the oxygen-iodine laser. The discharge was ignited between the coaxial electrodes with a radial distance of 3.5 mm in a flowing mixture of 0.1-0.9 $mmol.s^{-1}$ of CF_3I and 0.5-6 $mmol.s^{-1}$ of buffer gas (Ar, He) at a pressure of 2-3 kPa. The discharge stability was improved by different approaches so that the discharge could be operated up to a RF source limit of 500 W without sparking. The gas leaving the discharge was injected to the subsonic or supersonic flow of N_2 and concentration of generated atomic iodine and gas temperature were measured downstream of the injection. An inhomogeneous distribution of the produced iodine atoms among the injector exit holes was observed, which was attributed to a different gas residence time corresponding to each hole. The dissociation fraction was better with pure argon as a diluting gas than in the mixture of Ar-He, although the variation in the Ar flow rate had no significant effect on the CF_3I dissociation. The dissociation fraction calculated from the atomic iodine concentration measured several centimeters downstream of the injection was in the range of 7 to 30% when the absorbed electric energy ranged from 200 to 4000 J per 1 mmol of CF_3I. Corresponding values of the fraction of power spent on the dissociation decreased from 8 to 2%.% and the energy cost for one iodine atom increased from 30 to 130 eV. Due to a possible high rate of the atomic iodine loss by recombination after leaving the discharge, these values are considered as lower limits of those achieved in the discharge.

1. Introduction

The atomic iodine, an active species in the oxygen-iodine lasers, is traditionally produced in collisions of singlet oxygen with I_2 evaporated from either solid or liquid phase. It is supposed that a decomposition of a suitable gaseous iodine compound in the electric discharge may overcome the difficulties connected with I_2 usage and increase the laser efficiency [1,2].

Almost complete dissociation of CH_3I and HI was achieved by Mikheev et al [2], using a vortex stabilized DC glow discharge. There are, however, some disadvantages associated with these two donors. A carbon deposit is usually created on the electrodes when CH_3I is used, decreasing gradually the discharge stability and limiting thus the operation time [2]. This iodide has also low vapour pressure and must be heated-up for attaining higher flow rates, which may complicate the scaling-up of the device. The second donor, hydrogen iodide, is extremely corrosive and H atoms generated in the discharge may lead to the formation of unpleasant radicals in the oxygen environment.

Perfluormethyl iodide (CF_3I) is a promising donor of iodine atoms for iodine lasers. It is a stable, non-toxic and commercially available gas, which does not contribute to global warming [3]. Its first use in iodine lasers research is associated with the development of photodissociation iodine lasers. Pleasance and Weaver [4] first tried to replace common flash photolysis by a UV-initiated self-sustained discharge. They achieved a laser emission on the iodine $I(^2P_{1/2})$- $I(^2P_{3/2})$ transition and introduced two main processes of the electron impact on the CF_3I molecule:

$$CF_3I + e^- \rightarrow CF_3I^- + e^- \quad (1a)$$

$$CF_3I^- \rightarrow CF_3 + I^- \quad , \quad (1b)$$

and

$$CF_3I + e^- \rightarrow CF_3 + I \quad . \qquad (2)$$

Neither the rate coefficients nor the I/I^* ratio for was published in [4].
Thanks to its properties, CF_3I is of interest for the pulsed chemical oxygen-iodine laser. Since first experiments using the pulsed discharge in the O_2-CF_3I mixture [5], a thorough investigation of this system brought many new findings about relevant kinetics problems [6].
Quite recently, another production mechanism involving excited rare-gas atoms was pointed out in case of CH_3I [7,8]:

$$CH_3I + X^* \rightarrow CH_3 + I + X, \quad \rightarrow CH_3I^+ + X \quad k_3 = 1.3 \times 10^{-9}\ cm^3s^{-1}\ ,\ X = Ar, He \qquad (3)$$

with branching ratio 0.41 for the chemiionization (X = Ar) [8]. A similar process will probably occur in case of CF_3I.
A usage of CF_3I assisted by electrical discharge in the continuous-wave oxygen-iodine laser was not published yet. Such a method requires a simultaneous fulfillment of the following conditions: a/ the generation of I atoms must be as close as possible to the mixing point with singlet oxygen under sufficiently high pressure for the injection of decomposition products b/ these products must not quench the excited oxygen and iodine c/ the discharge effluent gas must not be too hot.
~~A relative rate~~Rates of the electron-impact processes (1) and (2) ~~is~~ are driven by the electron temperature. A traditional, low-pressure glow discharge with the electron temperature of 1-3 eV favors the process (2), which consumes electrons in the dissociative attachment. Therefore, such a discharge is often unstable and prone to arcing.
At higher pressures, recombination losses come into the play [~~7~~9]

$$CF_3 + I \rightarrow CF_3I\ ,\ ~~k_3~~k_4 = 1.54 \times 10^{-11}\ ~~cm^{-3}~~ \qquad ~~(3)~~cm^3s^{-1} \qquad (4)$$

$$I + I + M \rightarrow I_2 + M,\quad M = Ar, CF_3I, I_2 \quad . \qquad ~~(4)~~(5)$$

The rate coefficients at 300 K recommended in [10] are 8.06×10^{-33} cm^6s^{-2} (Ar) and 9.6×10^{-30} cm^6s^{-2} (I_2). The corresponding rate coefficient for M = CF_3I differ from 5×10^{-32} cm^6s^{-2} to 2.6×10^{-31} cm^6s^{-2} in the literature [9]. The back-recombination (~~3~~4) also competes with a dimerisation [~~7~~9]

$$2\,CF_3 \rightarrow C_2F_6\ ,\ ~~k_5~~k_6 = 1.04 \times 10^{-11}\ ~~cm^{-3}~~\ ; \qquad ~~(5)~~cm^3s^{-1}\ , \qquad (6)$$

which reduces to some extent the loss of atomic iodine ~~by~~in the process (~~3~~4).
Although the cross-sections of the processes (1,2) are large, due to a relatively low electron density in the electronegative discharge, the processes are not very fast, the rapid recombination (~~3~~4) slows down the net production process and limits the CF_3I dissociation fraction.
The early investigators were unable to produce iodine atoms by discharge decomposition in reasonable concentrations owing to a rapid recombination reaction on metal electrodes or on the wall of the discharge tube [~~8~~11]. Our approach is based on the idea [~~9~~12] of igniting the discharge inside the injector by which the iodine is delivered to the flow of excited oxygen in the oxygen-iodine laser. Using the RF discharge with a short inter-electrode gap, a small volume (several cm^3) and a short gas residence time (~100 μs) may be realized. The RF discharge gives its energy preferentially to electrons, while ions and neutrals remain cold in the fast flowing discharge. Non-equilibrium plasma with the electron temperature of few eV is created. The

concept of our discharge atomic iodine generator (DAIG) was published in ref. 1. In the next section, its realization in the experimental device is described in detail.

2. Experimental

A scheme of the apparatus is shown in figure 1.

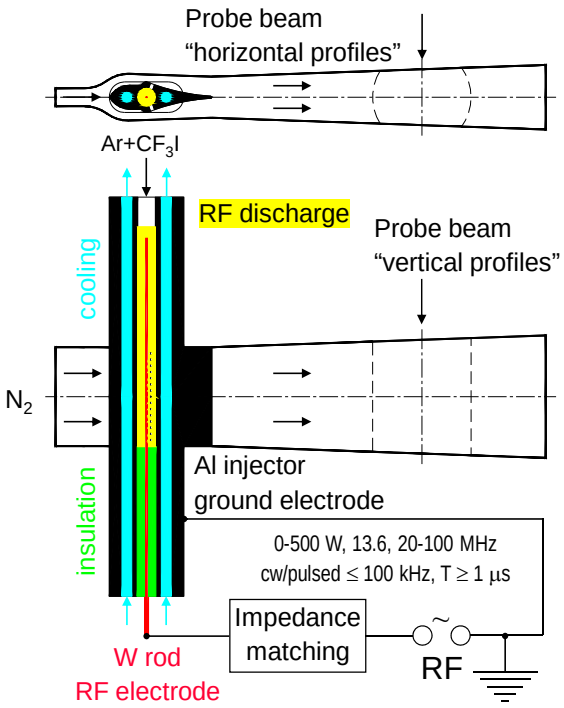

Figure 1. Simplified scheme of the experimental device.

The whole device was constructed to imitate a configuration of oxygen-iodine laser as close as possible. A central component made of pure aluminum (99.5% Al, A1050) combines the atomic iodine injector and an RF discharge chamber. Its outer shape was designed so that it formed, together with the cavity walls, a supersonic double-slit nozzle. A critical section of each half of the nozzle was 4 mm high and 50 mm wide. The discharge was sustained in the central cylindrical space of 9 mm inner diameter. The electrode length was 105, 95 or 60 mm. The left and right channels of 5 mm inner diameter served for introducing cooling water. The whole body was grounded, forming the second electrode.

The RF power source (Pearl Kogyo Co., Ltd, Osaka, Japan, model CF-500-20/100M) was a wideband tunable cw/pulse radiofrequency generator with oscillation frequency 20-100 MHz, output power ≤ 500 W, and a possibility to operate also in a repetitively pulsed mode with a repetition rate of 100 Hz – 99 kHz and pulse duty ratio of 5-95 %. By means of an L-type impedance matching circuit, a perfect matching was achieved at the RF frequency of 40 MHz, when the reflected power was below 1% of the forward power throughout all the experiments.

During the experimental run, the iodide was mixed with argon (0.5-4 mmol.s^{-1}) and/or helium (0-6 mmol.s^{-1}) and then introduced into the injector. The gas leaving the injector was mixed with N_2 (16–20 mmol.s^{-1}) flowing around the injector.

The flow rate of buffer gases He (99.996 %), Ar (99.998 %), and N_2 (99.998 %) (Air Products, Czech Republic) was derived from pressure drop on a needle valve (Swagelok, metering type, SS-4BMRW) maintained at a fixed, precisely defined opening position. A dependence of pressures upstream and downstream of the valve (measured by pressure transducers BHV, Czech Republic) on the molar flow rate measured by a mass flow meter (MKS, Germany, type 179A) was obtained using a particular working gas in a calibration procedure. The calibration was repeated for different needle valve opening and different upstream pressures. The results were correlated and the molar flow rates were calculated by the following equation

$$\dot{n} = a + b p_{up}^{0.5} \Delta p^{0.5} + c p_{up}^{-0.5} \Delta p^{1.5}, \qquad (7\cancel{6})$$

where $\Delta p = p_{up} - p_{down}$ and a,b,c are constants.

The flow rate of CF_3I (99%, Sigma Aldrich) was measured by a calibrated sonic orifice.
The discharge products were injected to the N_2 flow by two rows of orifices, either circular 2.2 mm in diameter or oval 2 mm wide and 3.3 mm long (see Section 3.2). The orifices were placed 4 mm downstream of the nozzle throat. The mixing of the injected gas with nitrogen, accelerated in the nozzle to a supersonic velocity (M~2), was periodically checked by the CFD calculations during the design procedure [\~~10~~13].
The pressure in the detection cavity was measured by a capacitive transducer (Leybold, Ltd.) placed 144 mm downstream of the injection point. By choking the flow far downstream by means of a butterfly valve, we could adjust the cavity pressure (130-900 Pa) and switch the flow from supersonic to subsonic one. Pressure in the discharge chamber was measured by a piezoelectric sensor (BHV, Czech Republic).
The PSI Iodine Scan Diagnostics (Physical Sciences Inc., USA, further labeled ISD, Physical Sciences, USA) employing a narrow band tunable diode probe laser was used for evaluation of atomic iodine concentration and temperature in the cavity. This instrument is monitoring the $I(^2P_{1/2})$ - $I(^2P_{3/2})$ transition of atomic iodine at 1315 nm [\~~11~~13]. The area of an absorption peak is directly proportional to the atomic iodine number density. The static gas temperature can be evaluated from the Doppler width of the peak after a de-convolution of the Voight fit of the line [\~~11~~13]. The ISD probe beam emitter/detector unit was mounted on the assembly of ~~a~~the motorized linear positioning equipment controlled by PC. The laser probe beam was led either in the 'top-bottom' direction and moved in parallel with the electrode (see the upper part of figure 1), or it was led in the 'side-to-side' direction and moved in the 'top-bottom' direction (see the lower part of figure 1). In these configurations, 'horizontal' and 'vertical' profiles, respectively, of atomic iodine number density and temperature were measured. These measurements were performed at several selected distances from the injection point (from 43 to 138 mm). While the 'vertical' profiles are important for a future laser application, 'horizontal' profiles are interesting for investigation of the processes in the discharge.
Atomic iodine concentration and temperature measured in the detection cavity were used for evaluation of the partial pressure of atomic iodine using the formula

$$p_I = \frac{1}{y_2 - y_1} \int_{y_1}^{y_2} c_I(y) R T(y) dy, \qquad (8\cancel{7})$$

where $c_I(y)$, $T(y)$ are the measured molar concentration and temperature, and y is the position in direction perpendicular or along the injector.
The dissociation fraction of CF_3I was evaluated using the formula

$$\eta_{diss} = \frac{p_I}{p_{cav}} \frac{\dot{n}}{\dot{n}_{RI}} \times 100\%, \qquad , \qquad (9\cancel{8})$$

where $\dot{n} = \dot{n}_{Ar} + \dot{n}_{He} + \dot{n}_{N2} + \dot{n}_{RI}$ is the total gas flow rate, and p_{cav} is the pressure in the detection cavity. ~~The equation (6)~~This evaluation of the dissociation fraction does not include excited iodine atoms, which may be formed in the discharge and eventually reach the detection region. Because the ISD signal absorption peak is proportional to c_I-$2c_{I^*}$, their presence will artificially decrease the dissociation fraction. The produced atomic iodine can also undergo its recombination (~~3~~4), (~~4~~5). Due to these facts, the value obtained by equations (~~7~~8), (~~8~~9) must be considered as a lower limit of the dissociation fraction yielded in the discharge.

The specific energy, E_{spec}, used in the summary evaluation of the results, was defined as

$$E_{spec} = P_{abs} / \dot{n}_{RI}\,, \qquad (~~9~~10)$$

where P_{abs} is the RF power absorbed in the plasma during the RI dissociation (evaluated by subtraction of the reflected power from the forward power) . While this parameter can be changed in several orders of magnitude, the total specific energy delivered to the discharge, $P_{abs}/(n_{iodide}+n_{Ar})$, was 30-150 J.mmol^{-1}.

The efficiency of the dissociation process was evaluated as a fraction of the absorbed RF power spent on the dissociation,

$$fP_{diss} = \frac{P_{diss}}{P_{abs}} = \frac{e\dot{N}_I E_{bond}}{P_{abs}}\,, \qquad (1~~0~~1)$$

where E_{bond} is the dissociation energy of C-I bond (2.34 eV.molec^{-1}), $\dot{N}_I$ is the evaluated flow rate of generated iodine atoms (in at/s), and e is the electric charge of electron.

3. Results

3.1 Injector with circular holes

Although the supersonic flow in the detection cavity is more relevant to the application in the laser and the low pressure suppresses the reactions which might occur from the holes exit to the detection place, mostly subsonic experiments were conducted. This was enforced by too low attenuation of the probe laser signal and the pressure had to be enhanced to 500-900 Pa. The effect of the pressure on the results is discussed in section 3.2.2.

3.1.1 Choice of buffer gas and basic dependencies

To begin with, the iodide was mixed with both argon and helium, and the influence of their relative content was examined. The dissociation fraction was calculated from vertical profiles of the ISD data according to equations (~~7~~8), (~~8~~9). It was found that a variation of the argon flow rate at the constant helium flow did not change the results significantly. On the other hand, when the mixture of Ar + He = 1.9 + 1.9 mmol.s^{-1} was replaced with 3.1 mmol.s^{-1} of Ar only, the dissociation fraction increased a lot. The situation is illustrated in figure 2 for different CF_3I flow rates. All dependences of dissociation fraction on the absorbed RF power in figure 2 are linear in the whole power range. The dissociation fraction is decreasing with increasing the CF_3I flow rate, but coming to higher flow rates, this decrease is slower.

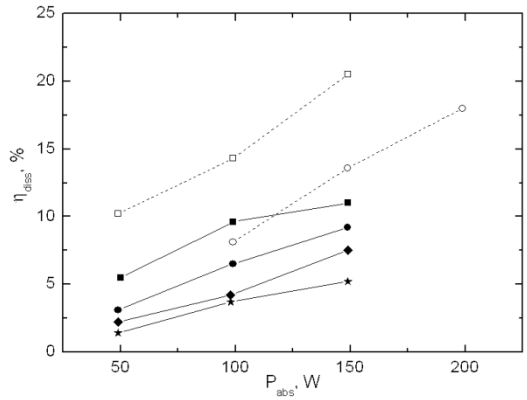

Figure 2. Dependence of the CF_3I dissociation fraction on the absorbed RF power and ~~CH_3I~~CF_3I flow rate, measured 138 mm downstream of the injector outlet. p_{cav} = 480-540 Pa; flow rates (in $mmol.s^{-1}$): 1.9 Ar + 1.9 He (solid lines), 3.1 Ar + 0 He (dashed line). CF_3I (in $mmol.s^{-1}$): 0.20 (■), 0.19 (□), 0.35 (●), 0.30 (○), 0.50 (◆), 0.70 (★).

Due to a choking of the flow on the injector exit holes and a relatively large mass fraction of CF_3I in the mixture, the discharge pressure was dependent on the gases flow rates and also on the RF power. The discharge pressure and other parameters for the selected experimental conditions are listed in table 1.

Table 1. Parameters of the selected experiments.
p_{disch} – pressure in the discharge chamber, V_{DC} – DC offset of RF voltage, η_{diss} – dissociation fraction

CF_3I $mmol.s^{-1}$	Ar $mmol.s^{-1}$	He $mmol.s^{-1}$	N_2 $mmol.s^{-1}$	p_{disch} kPa	P_{abs} W	V_{DC} V	η_{diss} %
0.19	3.09	0	20.4	1.88	49	-35	10.2
0.19	3.09	0	20.5	2.23	99	-83	14.3
0.21	1.96	2.04	20.5	2.32	99	-90	9.6
0.69	1.96	1.98	20.4	2.63	98	-45	3.7

From the first experiments, we concluded that a high ionization potential of helium is disadvantageous when working with a relatively high partial pressure of electronegative gas CF_3I and excluded it from subsequent experiments.

3.1.2 Distribution of atomic iodine among the injector exit holes

Utilizing a 'top-bottom' direction of the probe laser beam and moving it along the injector axis coordinate, we achieved horizontal profiles of the atomic iodine number density, which revealed the distribution of iodine atoms leaving individual holes of the injector. The distribution was asymmetric, increasing in the direction of the flow in the injector, and dependent on the electrode length~~,~~ (L_{elec}), which is evident from figure 3.

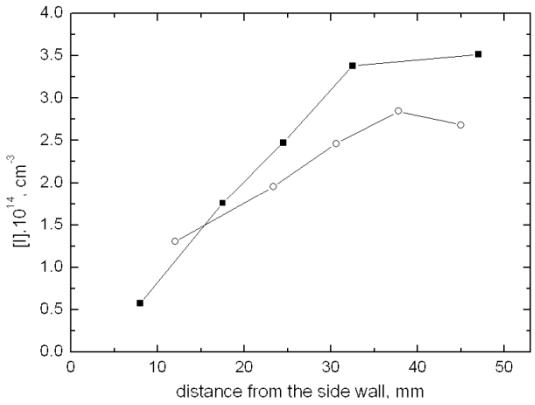

Figure 3. Horizontal profiles of atomic iodine number density 53 mm downstream of the injection. Conditions: (■): L_{elec} 60 mm, CF_3I 0.56 mmol.s^{-1}, Ar 2.25 mmol.s^{-1}, N_2 18.3 mmol.s^{-1}, p_{cav} 589 Pa, P_{abs} 147 W
(○): L_{elec} 105 mm, CF_3I 0.58 mmol.s^{-1}, Ar, 2.17 mmol.s^{-1} N_2, 21.3 mmol.s^{-1}, p_{cav} 651 Pa, P_{abs} 148 W

As can be seen in figure 1, the gas mixture flows a certain distance between the coaxial electrodes, then reaches the injection holes were it is gradually escaping from the discharge chamber and still smaller flow rate is being transported along the holes up to the last one. With the short electrode, having 60 mm in length, the gas molecules escaping by the first injection hole passed the discharge column 13 mm long only. As a result, almost no iodine atoms were injected out from the first hole. A subsequent steep rise of the iodine number density ejected from further holes is caused most probably by increasing residence time of gas in the discharge in this direction. This increase in residence time is higher than first order, since the flow is decelerating approaching the last hole. A residence time of the flow at conditions given in figure 3 between the 105 mm-long electrode tip and the first hole was much longer (0.47 ms) than for the short electrode version (0.14 ms), which yielded also more iodine atoms at first holes. The slope of the curve in figure 3 is smaller in the case of longer electrode, which could be ascribed to a lower power density in the longer discharge column. However, analyzing more experimental results, the dissociation fraction was approximately the same for both electrode lengths.

3.1.3 Temperature

The static temperature may be evaluated from the half-with of the Doppler component of the atomic iodine absorption peak measured by the ISD diagnostics. This evaluation is however very sensitive to the quality of the signal baseline and signal-to-noise ratio, which was rather low in the experiments. A comparison of the measurements under different conditions reveals that the temperature is dependent predominantly on the amount of the produced atomic iodine. In figure 4, the results with a long and short electrode are combined to one dependence of a temperature averaged over the cavity cross-section on the partial pressure of atomic iodine in the cavity.

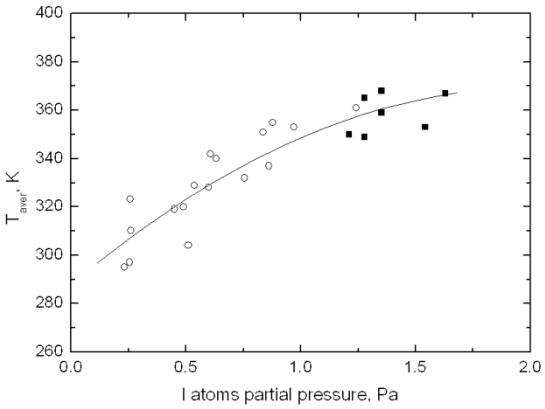

Figure 4. Dependence of the temperature averaged across the cavity cross-section, 61 mm downstream of the injection point, on the partial pressure of atomic iodine in the cavity. Different conditions, electrode length 60 mm (■), 105 mm (○).

This dependence is indicative of a chemical heat associated with the processes (4~~3~~) and (~~5~~6) that are very exothermic ($\Delta H_{f,3\text{-}4}$ = -223.4 kJ.mol^{-1} and $\Delta H_{f,5\text{-}6}$ = -403.4 kJ.mol^{-1}).

3.1.4 Discharge stability

The discharge was stable up to 150 W using the 60 mm long electrode and 200 W using the 105 mm long electrode, respectively. Beyond these values, a sparking was apparent at the exit of the injector holes, hindering further measurements. The discharge stability limit was enhanced by about 100 W utilizing a pulse-periodic mode of the RF source operation. In this case the dissociation fraction was similar to the cw mode at similar average power when the repetition frequency of 30 kHz and pulse duty ratio of 90% was applied.
In some experimental series the tungsten electrode was draped over by a fused quartz coating (a cylinder) of the inner and outer diameters 2 and 3.4 mm, respectively), to prevent sparking effects at higher RF powers. The discharge was then stable up to 400 W, even though small flow rates of CF_3I (0.07-0.14 mmol.s^{-1}) were examined only. The dissociation fraction was 37.8 % at 0.14 mmol.s^{-1} of CF_3I and 397 W of the absorbed power. The influence of the quartz cover on the dissociation fraction must be verified by further experiments.

3.2 Injector with oval holes

A theoretical consideration led us to a conclusion that better dissociation would be attained at a decreased pressure in the discharge chamber. It could be realized by enlarging the diameter of the injector holes. This would have also another positive effect on reducing the wall recombination of iodine atoms during their passage through the holes. However, for spatial reasons the diameter of the holes could not be further increased. Instead, the holes were extended only in the direction of primary flow. Such modified holes had an oval shape (rectangular with round ends in fact) and the width of 2 mm and the length of 3.3 mm. The cross-section of the original circular hole was thus increased by a factor of 1.5.
In the experiments with the modified holes and 95 mm long electrode, the discharge pressure was lower by about 20%. The discharge stability was much better than with the previous injector, so that the RF power up to the source limit (500 W) could be applied at a broad range of the flow rates of CF_3I (0.1-0.9 mmol.s^{-1}) and Ar (1.3-3.7 mmol.s^{-1}). Thanks to the excellent stability, a more relevant parametric study could be done. Also, due to higher achieved atomic iodine number densities, measurements at the supersonic flow conditions could be realized.

3.2.1 Vertical profiles of atomic iodine number density and gas temperature

The vertical profiles across the cavity height for three different flow rates of argon are shown in figure 5.

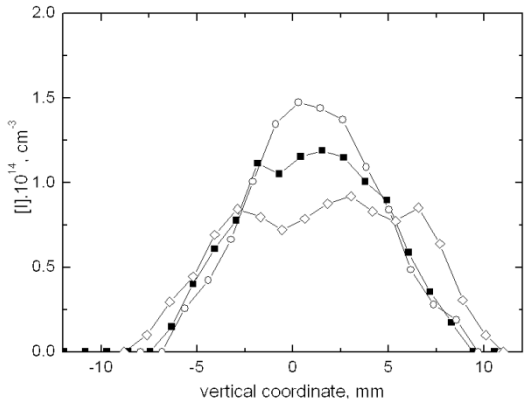

Figure 5. Vertical profiles of atomic iodine number density at different Ar flow rates measured 62 mm downstream of the injection. Supersonic flow, p_{cav} 128 Pa. Flow rates (in mmol.s^{-1}): 20 N_2, 0,15 CF_3I, Ar: 1.67 (○), 2.45 (■), 3.62 (◇); P_{abs} 397 W

It can be seen that the distribution of iodine atoms is homogenous across the cavity and the higher Ar flow broadens the distribution. The static temperature dropped off to 170-240 K at the points of maximum gas velocity (Mach number ~1.6). The maximum number density achieved in these experiments was 4.22 x 10^{14} cm^{-3} at the nozzle centerline. These results are promising with respect to using this method of the atomic iodine generation for the oxygen-iodine laser operation.

3.2.2 Dissociation fraction and production rate of I atoms

It was found that the variation in the static pressure in the cavity in the range of 128-504 Pa and in the distance from the injection plane from 61 to 111 mm, respectively, had no effect on the evaluated dissociation fraction. This founding indicates that the recombination losses of I atoms (~~34~~), (~~45~~) are not significant after (an) injection of the discharge products into the low-pressure nitrogen flow. A temperature dependence presented in section 3.1.3 may thus be caused by the fast and exothermic process (5).
The dissociation fraction and the flow rate of produced atomic iodine at the RF power of 400 W are plotted in dependence on the CF_3I flow rate in figure 6.

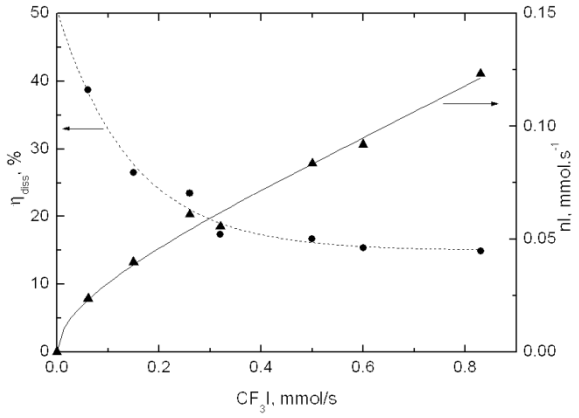

Figure 6. Dependence of the dissociation fraction (---) and I production rate (—) on the CF_3I flow rate. Ar 3.1 mmol.s^{-1}, N_2 20 mmol.s^{-1}, p_{cav} 128-130 Pa, P_{abs} 396-397 W.

It is interesting that the dissociation fraction is not decreasing at high values of CF_3I flow rates and remains ~15% within 0.4-0.83 mmol.s^{-1} of CF_3I. It means that the dissociation efficiency of the discharge was higher at higher iodide flow rate in the experiments. A maximum production rate of atomic iodine was 0.19 mmol.s^{-1} obtained at 0.9 mmol.s^{-1} of CF_3I and 495 W of the absorbed RF power.

3.2.3 Dependence on the specific energy

Due to the excellent discharge stability, we were able to change the specific energy parameter (equation ~~(9)~~10) in a very broad range from 250 J.mmol^{-1} to 5000 J.mmol^{-1}. In figure 7, a dependence of the dissociation fraction on the specific energy is shown together with results obtained in the experiments with the injector having the circular holes (two electrode lengths) and oval holes.

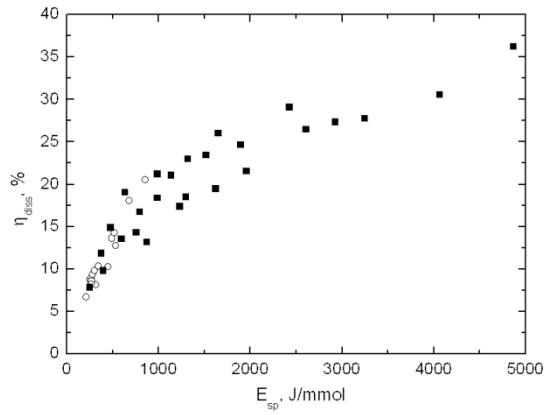

Figure 7. Dissociation fraction of CF_3I in dependence on specific energy, different conditions.
Injector holes: ○ - circular, ■ - oval

At low values of E_{spec}, there is no significant difference between the three examined configurations. A higher flow velocity in the discharge tube (i.e. a shorter residence time) may be the reason, why the dissociation fraction was not better at lower injector pressure (oval holes).

At higher E_{spec} > 2500 J.mmol^{-1}, the dissociation fraction increases with the specific energy very slowly. As it can be seen in figure 8, the discharge efficiency (evaluated from equation ~~(~~1~~0~~1~~)~~) falls down here to 2% only.

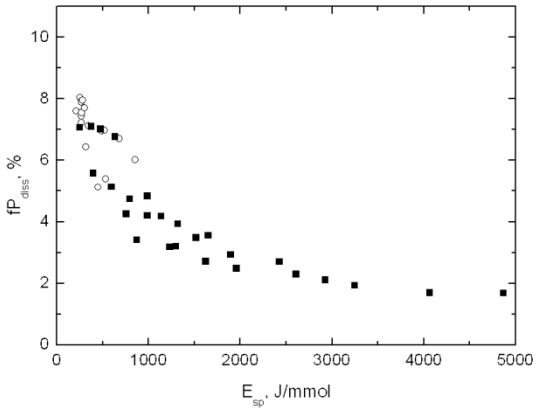

Figure 8. Fraction of RF power spent on the CF_3I dissociation in dependence on specific energy, different conditions. Injector holes: ○ - circular, ■ - oval.

4. Conclusions and final remarks

The generation of atomic iodine by dissociation of CF_3I in RF discharge was studied experimentally. The measurements showed that the distribution of atomic iodine was very inhomogeneous among the exit holes of the injector-discharge chamber, regardless ~~on~~of the gas flow rates and RF power, which was attributed to the fact that the outflow from each hole corresponds to a different gas residence time ~~corresponding to the gas flow through particular holes~~in the discharge. A worse initial discharge stability was improved by introducing different modifications of the device and experimental conditions. The enlargement of the injector exit holes was the most effective means.

A reasonable dissociation fraction (>30%) was achieved in the regions several centimeters downstream of the injection point at very high specific energy only, E_{spec} > 4 kJ per 1 mmol.s^{-1} of CF_3I. The CFD simulation [~~12~~15] showed that even 50% of the produced iodine atoms may be heterogeneously recombined on the passage through the injection hole, over the injector surface and, to less extent, homogenously on further way to the detection place. The real dissociation fraction achieved in the discharge is thus, probably, higher than our evaluation. The increasing number of iodine atoms along the injection holes but indicates that the mixture did not reach equilibrium composition and still better dissociation could be realized in the discharge.

The dissociation efficiency of the discharge was higher at higher iodide flow rate, and the maximum production rate of atomic iodine was 0.19 mmol.s^{-1} at 0.9 mmol.s^{-1} of CF_3I and 495 W of the absorbed RF power.

A 40 MHz-RF discharge ignited in the mixture of CF_3I + Ar is capable to generate iodine atoms at sufficiently high pressure for their injection into the supersonic flow of several hundred Pa. A possibility to attain quasi-homogeneously distributed number densities peaking at ~10^{15} cm^{-3} allows a usage of this method in continuous-wave supersonic oxygen-iodine lasers. A special attention must be paid however to potential reactions of molecular or atomic (in case of the discharge oxygen-iodine laser) oxygen with a residual, un-decomposed CF_3I, and also CF_3 radicals. For example, a CF_3O_2 radical produced in this way is a serious quencher of both singlet oxygen (k = 2.3 x 10^{-11} cm^{3}s^{-1}) and excited atomic iodine (2.5 x 10^{-11} cm^{3}s^{-1}) [~~13~~16].

Our device is capable to study the effects of these reactions on the operation of both chemical and discharge oxygen-iodine laser.

References

[1] Schmiedberger J, Jirásek V, Kodymová J, and Rohlena K 2009 *Eur. Phys. J.* D **54**, 239 - 248
[2] Mikheyev P A, Shepelenko A A, Voronov A I, and Kupryaev N V 2004 *J. Phys. D: Appl. Phys.* **37**, 3202-3206
[3] Solomon S, Burkholder J B, Ravishankara A R, Garcia R R 1994 *J. Geophys. Res.* **99** 20929
[4] Pleasance L D and Weaver L A 1975 *Appl. Phys. Lett.* **27**, 407
[5] Vagin N P, Pazyuk V S, Yuryshev N N 1995 *Quantum Electron.* **25**(8) 746-748
[6] Kochetov I V, Napartovich A P, Vagin N P, and Yuryshev N N 2009 *J. Phys. D: Appl. Phys.* **42** 055201
[7] Demyanov A V, Kochetov I V, Napartovich A P, Azyazov V N, and Mikheyev P A 2010 *Plasma Sources Sci. Technol.* **19** 025017
[8] Ionikh Y Z, Chernysheva N V 1994 Inelastic collisions of excited atoms of rare gases with molecules *Handbook Rate Constants of Elementary Processes with Atoms, Ions, Electrons and Photons* ed A G Zhiglinskiy (Saint-Petersburg: Saint-Petersburg State University), p 150,154 (in Russian)
~~[7]~~[9] NIST Chemical Kinetics Database,Version 7.0 (Web Version), Release 1.5
[10] Baulch D L, Duxbury J, Grant S J, and Montague D C 1981 *J. Phys. Chem. Ref. Data* **10** 576−635
~~[8]~~[11] Venugopalan M 1971 *Reactions under plasma conditions, Volume II* (Wiley-Interscience, John Wiley & Sons, Inc., USA) p 237-258
~~[9]~~[12] Schmiedberger J and Fujii H 2004 *Proc. SPIE* **5777**, 211-214
~~[10]~~[13] Jirásek V 2008 *Československý časopis pro fyziku* **58**(6) 383 – 387 (in Czech)
~~[11]~~[14] Tate R F, Hunt B S, Helms C A, Truesdell K A, and Hager G D 1995 *IEEE J. Quant. Electron.* **31** 1632-1636.
~~[12]~~[15] Jirásek V, Schmiedberger J, Čenský M, and Kodymová J 2009 *CD Proc. 40th AIAA Plasmadynamics and Lasers Conf.* (AIAA Paper 2009-4064)
~~[13]~~[16] Vagin N P, Zolotarev V A, Kryukov P G, Pazyuk V S, Podmar'kov Y~~u~~ P, Frolov M P and Yuryshev N N 1991 *Sov. J. Quantum Electron.* **21** 28

Acknowledgments

This work was supported by the Czech Science Foundation under the project No. 209/09/0310, and the European Office of Aerospace Research and Development (EOARD) under the Grant # FA8655-06-1-3034. The authors also thanks to the provider of the Academic Science Computing System LUNA for the possibility to perform parallelized CFD simulations.